


Chronic Stress Exposure Suppresses Mammary Tumor Growth and Reduces Circulating Exosome TGF- β Content via β -Adrenergic Receptor Signaling in MMTV-PyMT Mice

Breast Cancer: Basic and Clinical Research
Volume 14: 1–13
© The Author(s) 2020
Article reuse guidelines:
sagepub.com/journals-permissions
DOI: 10.1177/1178223420931511



Ryan P Dawes¹, Kathleen A Burke², Daniel K Byun², Zhou Xu², Petr Stastka³, Leland Chan³, Edward B Brown^{2*}  and Kelley S Madden^{2*}

¹Department of Neuroscience, University of Rochester Medical Center, Rochester, NY, USA.

²Department of Biomedical Engineering, University of Rochester, Rochester, NY, USA.

³Department of Biology, University of Rochester, Rochester, NY, USA.

ABSTRACT: Preclinical models of breast cancer have established mechanistic links between psychological stress and cancer progression. However, epidemiological evidence linking stress and cancer is equivocal. We tested the impact of stress exposure in female mice expressing the mouse mammary tumor virus polyoma middle-T antigen (MMTV-PyMT), a spontaneous model of mammary adenocarcinoma that mimics metastatic hormone receptor–positive human breast cancer development. MMTV-PyMT mice were socially isolated at 6 to 7 weeks of age during premalignant hyperplasia. To increase the potency of the stressor, singly housed mice were exposed to acute restraint stress (2 hours per day for 3 consecutive days) at 8 to 9 weeks of age during early carcinoma. Exposure to this dual stressor activated both major stress pathways, the sympathetic nervous system and hypothalamic–pituitary–adrenal axis throughout malignant transformation. Stressor exposure reduced mammary tumor burden in association with increased tumor cleaved caspase-3 expression, indicative of increased cell apoptosis. Stress exposure transiently increased tumor vascular endothelial growth factor and reduced tumor interleukin-6, but no other significant alterations in immune/inflammation-associated chemokines and cytokines or changes in myeloid cell populations were detected in tumors. No stress-induced change in second-harmonic generation-emitting collagen, indicative of a switch to a metastasis-promoting tumor extracellular matrix, was detected. Systemic indicators of slowed tumor progression included reduced myeloid-derived suppressor cell (MDSC) frequency in lung and spleen, and decreased transforming growth factor β (TGF- β) content in circulating exosomes, nanometer-sized particles associated with tumor progression. Chronic β -adrenergic receptor (β -AR) blockade with nadolol abrogated stress-induced alterations in tumor burden and cleaved caspase-3 expression, lung MDSC frequency, and exosomal TGF- β content. Despite the evidence for reduced tumor growth, metastatic lesions in the lung were not altered by stress exposure. Unexpectedly, β -blockade in nonstressed mice increased lung metastatic lesions and splenic MDSC frequency, suggesting that in MMTV-PyMT mice, β -AR activation also inhibits tumor progression in the absence of stress exposure. Together, these results suggest stress exposure can act through β -AR signaling to slow primary tumor growth in MMTV-PyMT mice.

KEYWORDS: Sympathetic nervous system, corticosterone, MMTV-PyMT, beta-adrenergic receptors, beta-blocker, myeloid-derived suppressor cells, exosomes, psychosocial stress

RECEIVED: January 8, 2020. **ACCEPTED:** March 12, 2020.

TYPE: Original Research

FUNDING: The author(s) disclosed receipt of the following financial support for the research, authorship, and/or publication of this article: This work was supported by National Cancer Institute Contract No. HHSN261200800001E, R21 CA152777-01, Department of Defense Breast Cancer Research Program (W81XWH-13-1-0439, W81XWH-10-01-008), University of Rochester Lung Biology Program NanoSight Pilot Grant to KSM; NINDS T32 NS007489T32, Breast Cancer Coalition of Rochester Breast Cancer Research Initiative Grant, University of Rochester Schmitt Program for Integrative Brain Research Seed Grant to RPD; Department of Defense Breast Cancer Research

Program (W81XWH-15-1-0040, W81XWH-09-1-0405, W81XWH-17-1-0011), NIH (DP2 OD006501-01, R21CA208921) to EBB. The funding agencies played no role in study design, data collection and analysis, decision to publish, or preparation of the article.

DECLARATION OF CONFLICTING INTERESTS: The author(s) declared no potential conflicts of interest with respect to the research, authorship, and/or publication of this article.

CORRESPONDING AUTHOR: Edward B Brown, Department of Biomedical Engineering, University of Rochester, RC Box 270168, Rochester, NY 14627, USA.
Email: Edward_Brown@urmc.rochester.edu

Introduction

Breast cancer is the most common invasive malignancy for women, with nearly 300,000 new diagnoses and 40,000 deaths from the disease in the United States each year.¹ Social isolation is associated with reduced long-term survival in all cancers, including breast cancer.² Preclinical studies have demonstrated that experimental stressors such as social isolation (single housing) or restraint increased breast cancer incidence and progression.^{3–8} Hypothalamic–pituitary–adrenal (HPA) axis and sympathetic nervous system (SNS) activation and subsequent β -adrenergic receptor (β -AR) signaling have been shown to drive tumor progression through immune and

nonimmune mechanisms.^{5–7,9–14} Nonetheless, epidemiological studies testing the association between stress and breast cancer progression in humans have been equivocal. Several groups have correlated significant life events, such as divorce or bereavement, with breast cancer mortality,^{15,16} whereas others have failed to identify such a link.¹⁷ In response to preclinical data demonstrating β -AR activation as a key mechanism underlying stress-induced tumor progression, breast cancer outcomes associated with β -blocker usage have been analyzed retrospectively. Several studies reported prolonged overall and breast cancer-specific survival and reduced establishment of secondary disease in patients taking β -blockers.^{16,18–21}

* Co-last authors



However, others show no such correlation,^{22–25} and 1 report demonstrated poorer outcomes associated with a selective β_1 -antagonist.²⁵ One roadblock to investigating stress and cancer progression in translational studies is that no stress-sensitive biomarkers have been identified to convey tumor stage and metastatic progression.

Circulating exosome content has been used as a biomarker reporting on tumor stage and metastasis.^{26–30} Exosomes constitute a class of nanometer-scale particles produced by the inward budding of the endosomal membrane. Nearly all cell types constitutively release exosomes following their fusion with the plasma membrane.³¹ In cancer, exosomes promote tumor growth and metastasis locally and distantly in metastatic sites.^{27,30–32} Exosomal transforming growth factor β (TGF- β) has been demonstrated to be an important mediator of tumor growth and progression, and elevated exosomal TGF- β content has been correlated with the onset of late-stage disease.^{33–35} Studies have demonstrated exosome content and function can be modified by stress neurohormone signaling,^{36,37} but the impact of such signaling in the context of cancer has yet to be investigated. As a first step in determining whether exosomes may serve as biomarkers of stress regulation of cancer, we investigated whether stress-induced alterations in tumor progression were associated with modifications of circulating exosome TGF- β content.

MMTV-PyMT female mice spontaneously develop hormone receptor-positive (estrogen/progesterone/Her2-Neu) ductal carcinoma, the most common clinical manifestation of breast cancer.^{1,38} We investigated the impact of stress exposure in this preclinical mouse model by initiating social isolation early in malignant transformation with subsequent exposure to acute restraint stress during early carcinoma. This dual stressor elicited pronounced activation of the SNS and the HPA axis throughout malignant transformation and, intriguingly, reduced primary tumor burden in MMTV-PyMT mice. Our investigation revealed tumor and systemic tumor pathways inhibited by β -AR activation, suggesting a need for further interrogation of stress hormone regulation of tumor progression in cancer.

Materials and Methods

Experimental animals

5- to 6-week-old female MMTV-PyMT (strain FVB/N-Tg(MMTV-PyVT)634Mul/J) mice were purchased from The Jackson Laboratory (Bar Harbor, Maine) and group-housed 4 per cage under microisolator conditions with a 12:12 hour light/dark cycle (lights on at 6:30 AM) and *ad libitum* access to food and water.

Stressor paradigm

After 2 weeks of habituation to group housing, mice were randomized into balanced “nonstressed” control or “stressed”

cohorts based on body weight and age (Figure 1A). Stressed animals were socially isolated (N = 1 per cage). Nonstressed controls remained group-housed throughout the experiment. Following 2 weeks of social isolation, stressed mice were exposed to 3 consecutive days of 2-hour restraint from 9 to 11 AM each day. Restraint tubes were well-ventilated 110-mL centrifuge tubes (Sigma-Aldrich, Z640948) that allowed mice to move forward/backward and turn around. After each restraint session, mice were returned to their respective cages. Nonstressed mice remained unrestrained in their home cages. Following the final restraint, mice were returned to their respective housing until they were sacrificed 24 hours, 2 weeks, or 3 weeks later. Mice were weighed 2 to 3 times per week throughout the paradigm. Animal handling was performed by the same experimenter (male, R.P.D.³⁹).

Chronic β -AR blockade with nadolol

Under isoflurane inhalation (3%–4% induction, 1%–2% maintenance, v/v oxygen), mice were implanted subcutaneously with 60-day continuous release pellets containing either placebo or the non-selective β -AR antagonist nadolol (1.5-mg per pellet; Innovative Research of America, Sarasota, FL) 3 days before social isolation. Nadolol was chosen in part because it does not cross the blood-brain barrier,⁴⁰ and the sustained release pellets remove the potential confound of exposing mice to stress associated with daily injections. The nadolol dosage was chosen based on previously reported effective doses of subcutaneously implanted nadolol pellets in mice.^{41,42} Nadolol is used in clinical populations, and has no intrinsic sympathomimetic or biased agonist activity.⁴⁰

Tissue collection

Mice were transferred to the procedure room, 1 cage at a time. Each mouse was weighed, bled via submandibular puncture into lithium heparin tubes (Sarstedt), and sacrificed by pentobarbital overdose and cervical dislocation within 5 minutes of removal from the housing room. MMTV-PyMT mice produce primary tumors in all mammary fat pads.³⁸ To assess total tumor burden, all solid mammary tumors were dissected and weighed. The largest solid tumors were subdivided for stress neurohormone, histological, cytokine/chemokine, and flow cytometric analyses. Spleens were weighed and divided for stress neurohormone and flow cytometry analyses. Lungs were removed and divided into half for histology and flow cytometry.

Plasma preparation

Whole blood was centrifuged at $2,000 \times g$ for 20 minutes at 22°C. Plasma for neurohormonal analysis was aliquoted and immediately stored at -80°C . Plasma for exosome isolation was immediately processed as described below.

Lung histology

One half of each lung was submerged in 10% buffered formalin for at least 24 hours prior to paraffin embedding. Lungs were sectioned at 5- μ m thickness, and 3 consecutive sections were collected every 100 μ m spanning the thickness of the lung. Sections were mounted onto glass slides (SurgiPath Xtra, Leica) and stained with hematoxylin and eosin (H&E). Metastases were counted, and the area of each metastatic lesion was measured by a blinded observer using a light microscope at 20 \times magnification.

Immunofluorescence and second-harmonic generation microscopy

Dissected tumors were fixed and immunolabeled as previously described.⁴³ For cleaved caspase-3 and Ki67 staining, heat-induced antigen retrieval using citrate buffer (Abcam) was conducted prior to blocking. Sections were labeled using anti-cleaved caspase-3 (1:100, Cell Signaling Technology) or anti-Ki67 (1:500, Abcam), followed by an AlexaFluor 594-conjugated goat anti-rabbit secondary antibody (1:500, Thermo Fisher). Slides were coverslipped with ProLong Gold antifade mountant with 4', 6-diamino-2-phenylindole nuclear stain (Thermo Fisher). Immunolabeled tumor sections were imaged on an Olympus BX51 upright microscope.⁴³

Collagen second-harmonic generation (SHG) microscopy was performed as previously described.⁴³ All image analyses were performed by blinded individuals using custom algorithms in ImageJ software (NIH).

Tumor cytokine/chemokine immunoassay

Tumors were homogenized in radioimmunoprecipitation assay (RIPA) buffer with HALT protease inhibitor (Thermo Fisher) and centrifuged at 1,000 \times *g* for 15 minutes. Cleared supernatants were aliquoted and stored at -80°C until use. Tumor lysates were assayed in duplicate for interleukin (IL)-1 β , IL-2, IL-4, IL-6, IL-10, IL-12(p70), interferon (IFN)- γ , granulocyte colony-stimulating factor (G-CSF), granulocyte-macrophage colony-stimulating factor (GM-CSF), macrophage colony-stimulating factor (M-CSF), monocyte chemoattractant protein (MCP-1), macrophage inflammatory protein (MIP)-2, regulated on activation normal T-cell expressed and secreted (RANTES), tumor necrosis factor (TNF)- α , and vascular endothelial growth factor (VEGF) by a multiplexed immunoassay (EMD Millipore, MCYTOMAG-79K) and analyzed on a BioRad BioPlex 200 array reader. Analyte concentrations were determined from standard curves using 5-point logarithmic fit.

Analytical flow cytometry

Tissue was placed in ice-cold phosphate-buffered saline (PBS) with 10% fetal bovine serum (FBS) and manually dissociated

into single-cell suspensions in PBS with 10% FBS. Red blood cells were lysed in buffer containing 0.15 M ammonium chloride, 10 mM potassium carbonate, and 0.1 mM sodium ethylenediaminetetraacetic acid in distilled/deionized water (pH 7.4). Cell suspensions were filtered through 70- μ m cell strainer cap tubes (Corning). Cells (1×10^6) were Fc-blocked by a 15-minute incubation with anti-CD16/32 (1:50, BD Biosciences) and labeled with the following antibody panel: anti-CD45 (Brilliant Violet 421, Biolegend, 30-F11); -CD11b (AlexaFluor647, BD Biosciences, M1/70); -Gr-1 (Ly-6C & -6C, PE, BD Biosciences, RB6-8C5); and -F4/80 (FITC, Abcam, BM8), all diluted 1:40 in PBS with 1% bovine serum albumin (BSA) for 30 minutes at 4°C. Following 3 washes in PBS with 1% BSA, cells were fixed in 1% paraformaldehyde and stored at 4°C until analysis.

Cells were analyzed using a BD Biosciences FACSCanto II cytometer. Color compensation was conducted for each fluorescent channel using antibody capture beads (Life Technologies). Analysis gates were set based on forward-scatter/side-scatter profiles to exclude debris and fluorescence-minus-one negative controls.⁴⁴ Flow cytometric analyses were performed in FlowJo X (Tree Star).

Exosome isolation

Immediately after plasma preparation, exosomes were collected using an ExoQuick Plasma Exosome Isolation kit per manufacturer instructions (System Biosciences, EXOQ5™). In brief, debris and nonexosomal particles were removed by a 15-minute incubation with thrombin at 37°C followed by centrifugation at 10,000 \times *g* for 20 minutes. ExoQuick precipitation solution was added to each supernatant (1/3 v/v) and mixed by inversion. Samples were incubated overnight at 4°C and pelleted by centrifugation at 10,000 \times *g* for 30 minutes at 4°C. The exosome-depleted supernatant was removed and the pellet was centrifuged at 10,000 \times *g* for an additional 5 minutes at 4°C to remove remnant supernatant and ExoQuick reagent. Pellets were resuspended in sterile Dulbecco's PBS (Corning) for size distribution and transmission electron microscopy (TEM) morphological analyses or sonicated in RIPA buffer with HALT protease inhibitor cocktail (Thermo Fisher) for protein analysis, then stored at -80°C.

Exosome size determination

Exosome diameter was determined by TEM and NanoSight particle tracking analysis. For TEM, undiluted exosomes were adsorbed onto formvar/carbon-coated copper grids, counterstained with uranyl acetate, and imaged at 50,000 \times and 150,000 \times magnification using a Hitachi 7650 analytical TEM paired with an 11-megapixel Erlangshen digital camera. For NanoSight size distribution analysis, exosomes were diluted 1:1,000 in molecular grade water (Corning, 46-000-CM) and analyzed using a NanoSight NS300 (NTA version 3.1, Malvern).

For all samples, camera level=12, frame rate=25 FPS, acquisition time=3×60 seconds, viscosity=water (~0.9 cP), detection threshold=5, blur size=auto, max jump distance=auto.

Exosome protein analysis

Total exosome protein was assayed by bicinchoninic acid assay (Thermo Fisher). Isolated particles were confirmed as exosomes by the presence of common surface markers and the absence of cellular contamination using an ExoCheck antibody-based spot array (System Biosciences, EXORAY). The exosome number was estimated using the canonical marker CD63⁴⁵ by enzyme-linked immunosorbent assay (ELISA; System Biosciences, EXOEL-CD63A). Exosomal TGF- β 1/2/3 protein expression was assayed by multiplexed immunoassay (EMD Millipore, TGF β MAG-64K). Exosomal TGF- β concentrations are expressed as pg per 1×10^9 CD63⁺ particles.

R221a cells, intracellular cyclic adenosine monophosphate, and proliferation

The MMTV-PyMT-derived cell line R221a was maintained in Dulbecco's modified Eagle's medium supplemented with 10% FBS, 1% penicillin/streptomycin, 50- μ g/mL gentamycin, and 10- μ g/mL puromycin.⁴⁶ Intracellular cyclic adenosine monophosphate (cAMP) was measured by ELISA as previously described.⁴⁷ Cellular proliferation was assessed using a CyQUANT NF Cell Proliferation Assay kit (Molecular Probes).

Neuroendocrine determination

Tissue was homogenized in 0.01 M hydrochloric acid at 10% w/v and centrifuged at $1,000 \times g$ for 15 minutes to remove cellular debris. Supernatant was stored at -80°C until analysis. The norepinephrine (NE) metabolite normetanephrine (NMN) was assayed by ELISA (BA E-8200, Rocky Mountain Diagnostics). Normetanephrine concentrations were normalized to wet tissue weight. Plasma corticosterone was measured by ELISA (MS E-5400; Rocky Mountain Diagnostics).

Statistical analysis

All statistical analyses were performed with Prism 6 (GraphPad Software). For the time course experiment comparing nonstressed with stressed groups, $n=16$ per group as dictated by *a priori* power analysis of tumor burden. For the nadolol experiment with 4 experimental cohorts, $n=8$ per group. Statistical outliers were identified using the ROUT outlier test. Significant main effects or interactions revealed by 2-way analysis of variance (ANOVA) were followed up post hoc by Holm-Sidak multiple comparison or by 2-tailed student's t test. For 2-group comparisons, statistical differences were determined by unpaired, 2-tailed student's t test. Statistical differences in body

weight over time were determined with repeated measures 2-way ANOVA and Holm-Sidak multiple comparison post hoc test. Fisher exact test was used to compare frequency of lung metastatic lesions. Pearson correlation analysis was used to calculate F tests and determine significant deviations from slope=0 ($P < .05$).

Results

Characterization of experimental stress exposure in MMTV-PyMT mice

To study the impact of exposure to stress on mammary tumor growth in the transgenic MMTV-PyMT mouse line, we initially tested social isolation which has been reported to increase mammary tumor growth in other preclinical mammary tumor models.^{3-6,8} However, social isolation tested at different ages and durations did not significantly modify tumor growth in MMTV-PyMT mice (data not shown). Motivated by reports demonstrating heightened stress neurohormonal responses in isolated mice exposed to an acute stressor,^{3,4,48,49} we socially isolated mice during premalignant hyperplasia and then exposed them to a short-term restraint stress during early carcinoma,^{49,50} as detailed in the "Materials and Methods" section and diagrammed in Figure 1A. In developing the parameters of the acute restraint stressor, we sought to avoid long-term weight loss, such as that induced by homotypic restraint stress alone.⁵¹ In the week following social isolation, mice failed to gain body weight as compared with the nonstressed, group-housed mice (Figure 1B), but the stressed mice recovered body weight until there was no difference immediately after restraint stress (Figure 1B; main effect of stress, $P = .01$; time, $P < .0001$; Stress \times Time Interaction, $P < .0003$). In MMTV-PyMT mice, palpable solid tumors are detectable only after 8 to 9 weeks of age; therefore, these early changes in body weight are independent of solid tumor development.

Stress exposure activated SNS and HPA axis

To characterize the neurohormonal response elicited by exposure of socially isolated MMTV-PyMT mice to restraint stress, SNS and HPA axis activation was assessed 24 hours, 2 weeks, and 3 weeks after the final restraint session in separate groups of mice. Plasma CORT, an indicator of HPA axis activation, was significantly elevated at all 3 time points compared with the corresponding nonstressed group (Figure 1C; main effect of stress, $P < .0001$; time, $P = .8$; Stress \times Time Interaction, $P = .8$). To assess SNS activation, NMN, a metabolite of NE, was measured in tumors and spleen.^{43,52,53} In the spleen, stress exposure significantly increased NMN (Figure 1D; main effect of stress, $P < .0001$; time, $P < .0001$; Stress \times Time Interaction, $P = .3$). In tumors, NMN did not differ between nonstressed and stressed mice at any time point (main effect stress, $P = .3$; Stress \times Time Interaction, $P = .9$),

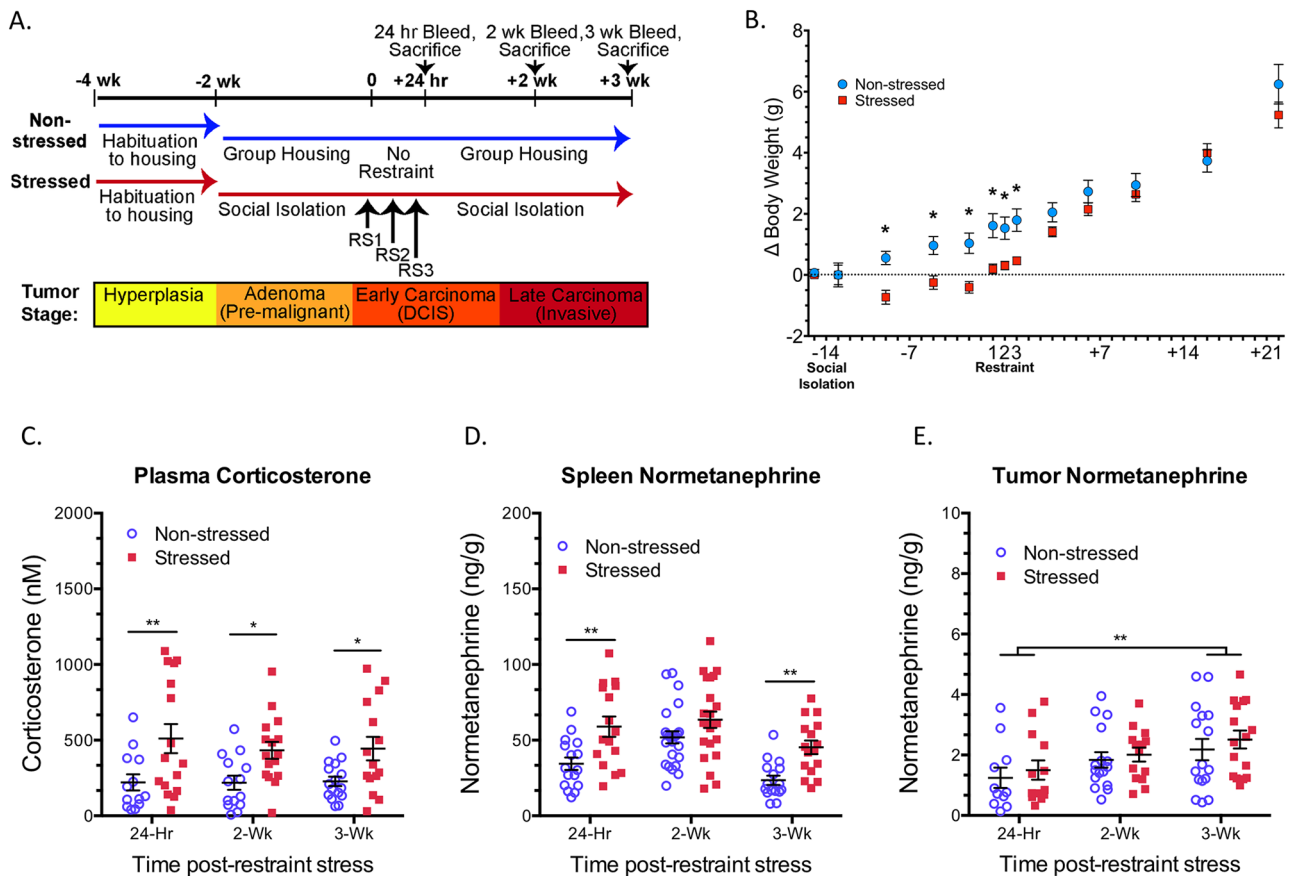


Figure 1. HPA axis and SNS activation with the dual stressor paradigm in MMTV-PyMT mice. (A) Diagram of dual stress paradigm. In the stressed group, group-housed mice were singly housed during hyperplasia at 6-7 weeks of age. At 8-9 weeks of age, during early carcinoma, singly-housed mice were exposed to 3 consecutive days of 2 h per day restraint stress (RS). Non-stressed mice were group-housed remained group-housed throughout the experimental period. (B) Change in body weight (Δ) relative to 1 day before social isolation. The stress neurohormones (C) plasma corticosterone, (D) spleen normetanephrine, and (E) tumor normetanephrine were measured at 3 time points after the last restraint stress session. Individual responses are shown in C-E. Results are expressed as mean \pm SEM, $n=14-16$. Statistical analyses: Fig 1B-D, Holm-Sidak multiple comparison-adjusted post-hoc test comparing non-stressed and stressed groups at the corresponding time points. * $p<0.05$ or ** $p<0.01$. For Fig. 1E, post-hoc analysis of main effect of time, ** $p<0.01$ between 24 h and 3-wk time points by Holm-Sidak multiple comparison test.

but a significant effect of time was noted ($P=.01$; Figure 1E). Post hoc analysis revealed tumor NMN was significantly greater at 3 weeks compared with 24-hour post-restraint stress, independent of stress exposure.

Stress suppressed tumor growth, but not metastasis

To evaluate the impact of stress on tumor growth, tumor burden (weight of all solid tumors) was measured at 24 hours, 2 weeks, and 3 weeks after the final restraint session in the same mice as in Figure 1. Unexpectedly, tumor burden was reduced by stress exposure (Figure 2A; main effect of stress, $P=.007$; time, $P<.0001$; Stress \times Time Interaction, $P=.066$) by 50% (Holm-Sidak, $P<.05$) at the 2-week time point and by 30% (Holm-Sidak, $P=.05$) at the 3-week time point.

Metastatic lesion number and size were determined in H&E-stained lung tissue sections (Figure 2B), the primary metastatic site in MMTV-PyMT mice.³⁸ No lung metastatic lesions were detected at 24 hours post-restraint in either

group as expected at this age.³⁸ At 2 weeks post-restraint, no difference in the frequency of mice with metastatic lesions was detected between nonstressed and stressed mice (5 of 16, nonstress group; 4 of 15, stress group; Fisher exact test, $P=1.0$). At 3 weeks post-restraint, all mice presented with lung metastases. In mice with detectable metastatic lung lesions, the number of lung metastases did not differ between the nonstressed and stressed groups (Figure 2C; main effect of stress, $P=.7$; time, $P=.08$; Stress \times Time Interaction, $P=.5$). The size of metastatic lesions was greater in stressed mice 2 weeks, but not 3 weeks, post-restraint (Figure 2D; main effect of stress, $P=.02$; time, $P=.3$; Stress \times Time Interaction, $P=.02$).

Mechanisms of stress-induced tumor inhibition

In light of the unexpected tumor-suppressive effects of the stressor, we sought to identify stress-sensitive tumor pathways that slowed tumor growth in MMTV-PyMT mice.

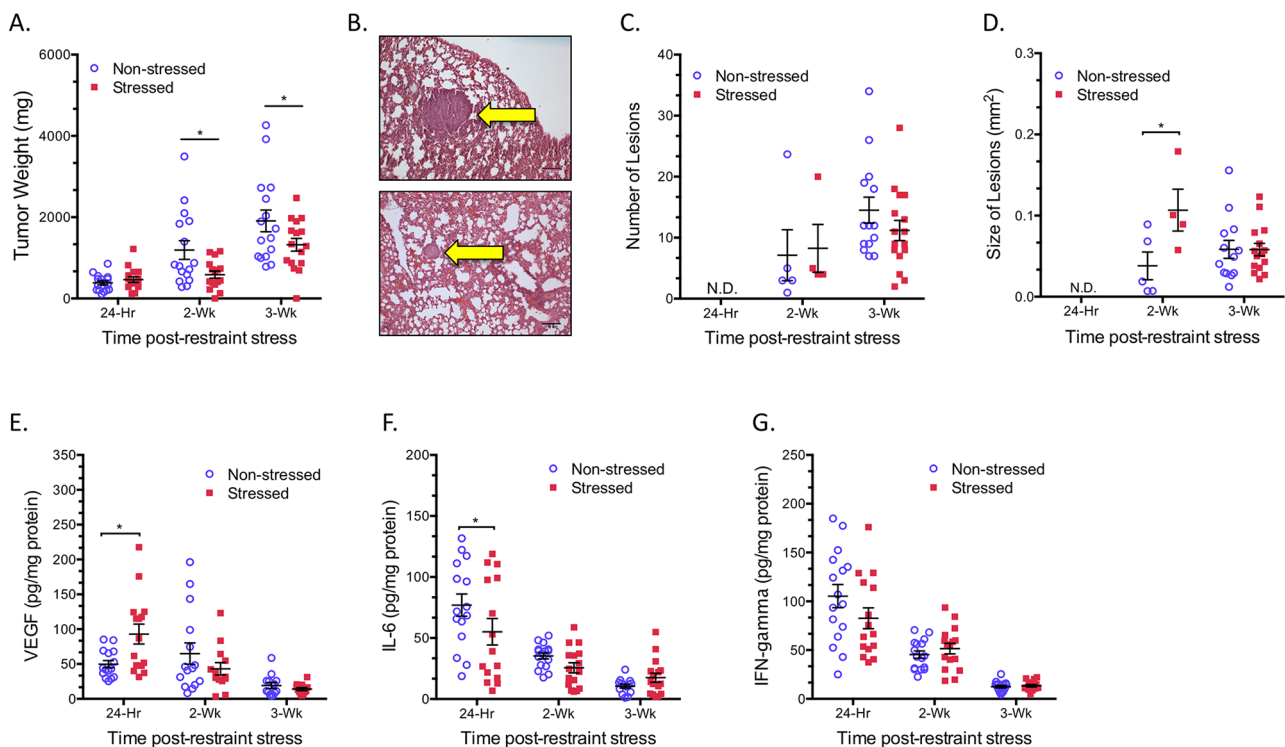


Figure 2. Stress exposure suppresses primary tumor growth, but does not alter lung metastasis in MMTV-PyMT mice. (A) Total tumor burden at 3 time points after restraint stress. (B) Representative images of H&E-stained lung tissue sections from 2 MMTV-PyMT mice. 10X magnification; scale bars = 100 μ m. Yellow arrows indicate metastatic lesions. Quantification of (C) number and (D) size of metastatic lesions from H&E stained lung sections. Tumor concentration of (E) VEGF; (F) IL-6, and (G) IFN- γ . Individual responses are indicated. Results are expressed as mean \pm SEM. Statistical analyses: Holm-Sidak multiple comparison post-hoc test comparing non-stressed and stressed groups at the corresponding time points, * $p < 0.05$; N.D.= not detectable.

Hypothalamic-pituitary-adrenal axis activation and glucocorticoids can suppress immune and inflammatory cytokines and chemokines known to regulate tumor growth.⁵⁴ Three important tumor cytokines, the proangiogenic VEGF, pro-inflammatory cytokine IL-6, and IFN- γ , a key T cell-derived cytokine effector of antitumor immunity were significantly modified over time (Figure 2E to G; main effect of time, $P < .0001$). However, each cytokine varied in its stress responsiveness. Vascular endothelial growth factor increased transiently with stress exposure (Figure 2E; main effect stress, $P = .5$; Stress \times Time Interaction, $P = .005$). A trend toward reduced IL-6 (Figure 2F; stress, $P = .1$; Stress \times Time Interaction, $P = .08$) was detected. Interferon- γ was not modified with stress exposure (Figure 2G; stress, $P = .4$; Stress \times Time Interaction, $P = .1$). No other tumor cytokines and chemokines, including IL-1 β , IL-2, IL-4, IL-10, IL-12(p70), G-CSF, GM-CSF, M-CSF, MCP-1, MIP-2, RANTES, and TNF- α , were significantly altered by stress exposure (data not shown).

To probe other tumor inhibitory mechanisms, infiltrating immune cells, cell proliferation, and the extracellular matrix were examined in tumors from stressed and nonstressed mice. Two stress-sensitive immunosuppressive myeloid populations, CD11b⁺Gr-1⁺ myeloid-derived suppressor cells

(MDSCs) and CD11b⁺F4/80⁺ tumor-associated macrophages (TAMs), were assessed by flow cytometry.^{5,8} Representative gating on CD45⁺ leukocytes to exclude CD45-negative tumor cells is depicted in Supplemental Figure 1. Tumor MDSC and TAM frequency increased over time (time, $P < .0001$); however, stress exposure did not alter MDSC or TAM frequency at any time point (Figure 3A MDSC: stress, $P = .5$; Stress \times Time Interaction, $P = .7$; Figure 3B TAM: stress, $P = .1$; Stress \times Time Interaction, $P = .4$). Similarly, neither the frequencies of T cells (CD4, CD8, CD25⁺/FoxP3⁺ Treg) nor those of natural killer cells (CD49b, CD69) were modified by stress exposure 2 weeks post-restraint (data not shown). Stress exposure also did not significantly alter the frequency of proliferating cells within the tumor as determined by Ki67 immunoreactivity at 2 weeks post-restraint (t test, $P = .13$, Supplemental Figure 2A). To assess stress sensitivity of the tumor extracellular matrix, we quantified SHG-emitting tumor collagen. We had previously shown in orthotopic mammary tumors that tumor SHG is altered in association with elevated tumor NE in mice and with tumor progression in human breast cancer.^{43,55} Stress exposure did not alter SHG-emitting fibrillar collagen in MMTV-PyMT tumors (stress, $P = .3$; Stress \times Time Interaction, $P = .15$), but changes in SHG with tumor

progression over time were readily detected ($P < .0001$; Supplemental Figure 2B). Together, these results indicated stress exposure blunted tumor growth without significantly modifying key components of the tumor microenvironment.

Systemic responses to tumor suppression: reduced MDSCs and circulating exosome TGF- β content

In MMTV-PyMT mice, MDSCs and TAMs increased in the spleen and lung with advancing tumor stage (Figure 3C to F; main effect of time, $P < .0001$). Furthermore, in

association with reduced tumor burden, stress exposure reduced MDSC frequency in the spleen (Figure 3C; stress, $P = .004$; Stress \times Time Interaction, $P = .03$) and lungs (Figure 3E; stress, $P = .6$; Stress \times Time Interaction, $P = .014$) at 2 weeks post-restraint. Stress exposure did not alter the frequency of TAMs in the spleen (Figure 3D; stress, $P = .3$; Stress \times Time Interaction, $P = .09$) or lung (Figure 3F; stress, $P = .7$; Stress \times Time Interaction, $P = .7$) and post hoc analysis revealed no differences at any time point.

To further evaluate potential stress-induced alterations to the systemic environment, we also isolated and characterized

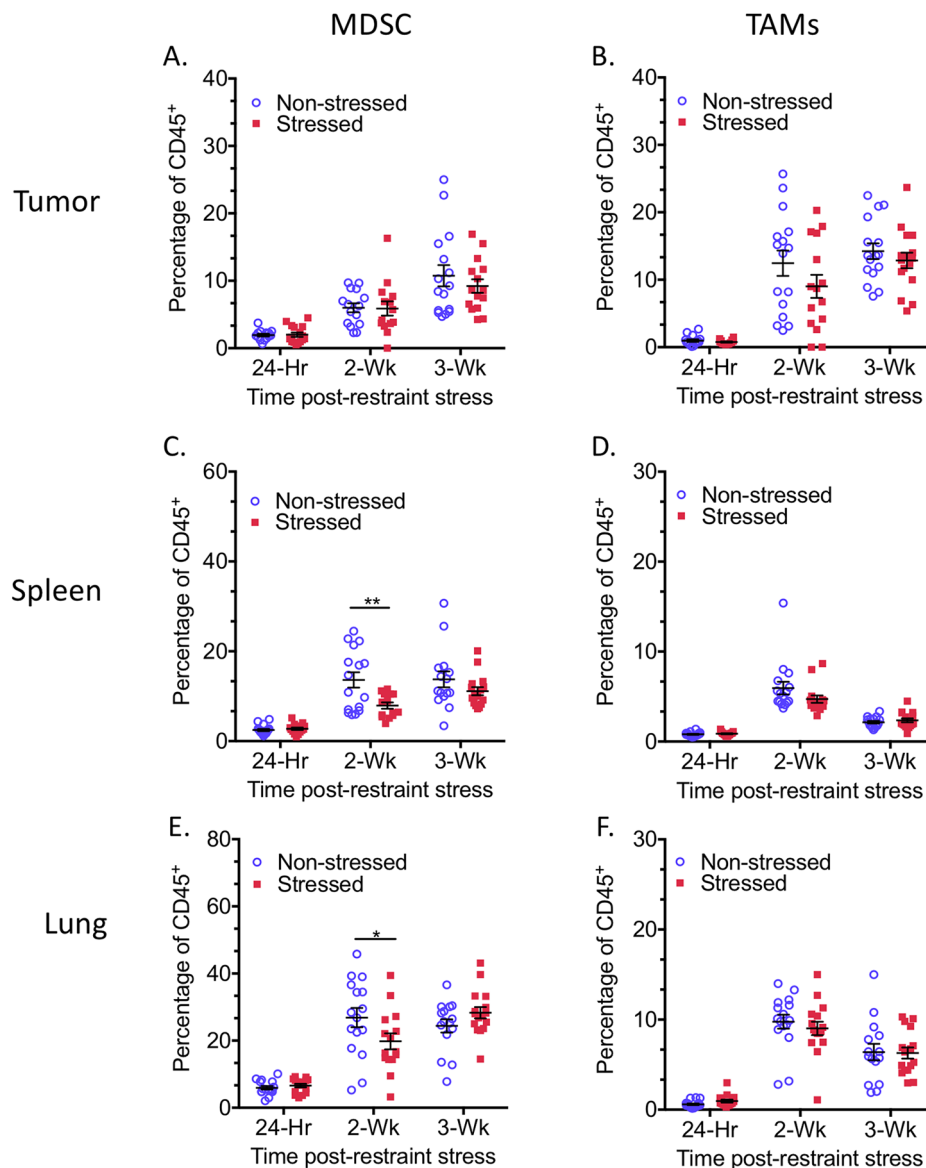


Figure 3. MDSC frequency and TAM frequency in tumor, spleen and lung. (A, C, E) MDSC and (B, D, F) TAM in (A, B) tumor, (C, D) spleen, and (E, F) lung at 3 time points after restraint stress. Individual responses are indicated. Results are expressed as mean \pm SEM. Statistical analyses: Holm-Sidak multiple comparison post-hoc test comparing non-stressed and stressed groups at the corresponding time points,* $p < 0.05$; ** $p < 0.01$

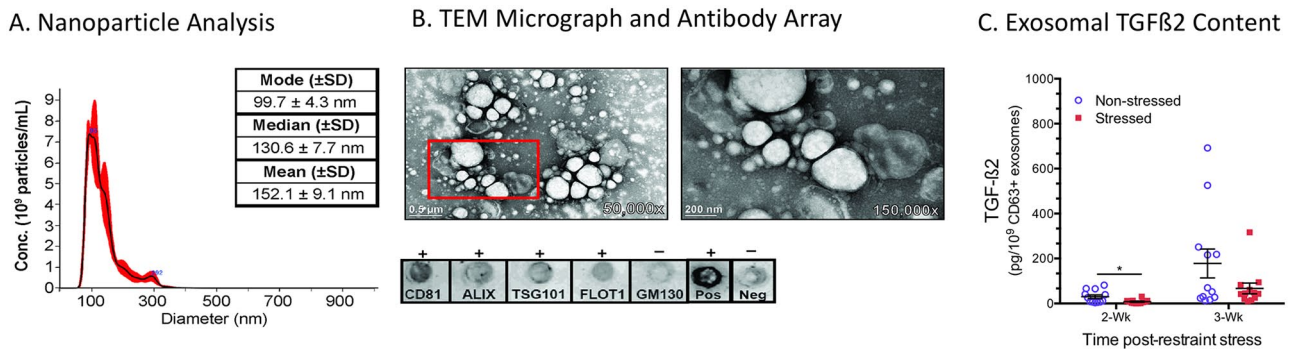


Figure 4. Plasma Exosome Isolation and TGF β Content. (A) Analysis of nanoparticle diameter; (B) Transmission electron microscopy (TEM) and antibody array of expressed proteins indicating lack of cellular contamination, (C) Exosomal TGF β content 2-wk and 3-wk after restraint stress. Individual responses are indicated. Results are expressed as mean \pm SEM. Statistical analyses: Holm-Sidak multiple comparison post-hoc test comparing non-stressed and stressed groups at the corresponding time points,* $p < 0.05$.

circulating exosomes, disseminated extracellular vesicles that report on and facilitate tumor progression.^{26,29,30,33} Based on nanoparticle tracking analysis and TEM, isolated exosomes exhibited the spherical morphologies and diameters of approximately 100 nm expected for unfixed exosomes (Figure 4A and B).³¹ The isolated exosomes expressed classical surface markers, including CD81, Alix, tumor-suppressor gene 101 (TSG101), and flotillin-1 (FLOT1), but not the golgi-associated protein GM130, indicating cellular contamination was not present (Figure 4B). Exosomal IL-6, IFN- γ , IL-1 β , IL-2, IL-4, IL-10, IL-12(p70), G-CSF, GM-CSF, M-CSF, MCP-1, MIP-2, RANTES, VEGF, and TNF- α were at or below the level of detection (data not shown). On the other hand, TGF- β 2 content was detectable in exosomes at 2 weeks, and it increased between 2 and 3 weeks post-restraint (main effect of time, $P = .004$; Figure 4C). Stress exposure reduced exosome TGF- β 2 content in CD63+ exosomes (stress, $P = .05$; Stress \times Time Interaction, $P = .2$) 2 weeks post-restraint (Holm-Sidak, $P < .05$). Exosomal TGF- β 1 was not modified by stress, and TGF- β 3 was not detectable in most mice (data not shown).

β -AR blockade with nadolol abrogated stress-induced tumor suppression

A correlation analysis revealed that splenic NMN (a surrogate measure of peripheral SNS activation) was inversely correlated with tumor burden at the 2 week time point (Supplemental Figure 3A; Pearson correlation, $R^2 = 0.077$, $P = .006$), implicating increased SNS outflow as a driver of suppressed tumor growth in MMTV-PyMT mice. Furthermore, a tumor cell line (R221a) derived from MMTV-PyMT tumors⁴⁶ was sensitive to the non-selective β -AR agonist isoproterenol, as measured by elevated intracellular cAMP (Supplemental Figure 3B), suggesting that MMTV-PyMT tumor cells are responsive to β -AR stimulation. Therefore, to determine whether sympathetic activation mediates stress-induced tumor suppression through β -AR signaling, mice were

implanted with the non-selective β -AR antagonist nadolol to achieve peripheral β -blockade throughout the stress paradigm.

Body weight recovered more rapidly after social isolation in stressed mice treated with nadolol, compared with placebo-treated stressed mice (Figure 5A; stress, $P = .017$; time, $P < .0001$; Stress \times Time Interaction, $P < .002$). Tumor burden assessed 2 weeks post-restraint was reduced 48.5% in placebo/stressed mice (Figure 5B) compared with placebo/nonstressed mice, but by 2-way ANOVA, no significant effect of stress and no stress by nadolol interaction were detected. Nonetheless, the 48.5% reduction in tumor burden was equivalent to the 49.2% reduction observed in stressed mice in Figure 2A with $n = 16$. Tumor burden in placebo-treated stressed mice was significantly reduced compared with placebo-treated nonstressed mice (t test, $P = .049$). Furthermore, tumor burden in nadolol-treated stressed mice was significantly greater than placebo/stressed mice (t test, $P = .02$) and was equivalent to placebo/nonstressed mice (Figure 5B; t test, $P = .5$) indicating that β -blockade prevented the stress effect. To test whether the stress-induced decrease in tumor burden was associated with increased cellular apoptosis, tumor cleaved caspase-3 was detected by immunohistochemical staining (Supplemental Figure 4).⁵⁶ Cleaved caspase-3 staining was significantly elevated in placebo/stressed mice compared with all other groups, indicating β -blockade prevented the stress-induced increase in apoptosis (Figure 5C, stress, $P = .17$; Stress \times Nadolol Interaction, $P = .047$). Together, these results demonstrate stressor exposure reduced tumor burden and increased tumor-associated apoptosis through β -AR signaling.

Stressor exposure did not alter the number of metastatic lesions (Figure 5D; stress, $P = .4$, interaction, $P = .25$), lesion area (Figure 5E, stress, $P = .43$; Stress \times Nadolol Interaction, $P = .07$), tumor MDSCs (Figure 5F, stress, $P = .9$; Stress \times Nadolol Interaction, $P = .4$), or TAM frequency (Figure 5G, stress, $P = .9$; Stress \times Nadolol Interaction, $P = .5$). In the lung, the stress-induced reduction of MDSC frequency was prevented by nadolol treatment (Figure 5H, stress, $P = .11$; Stress \times Nadolol Interaction, $P = .019$). Lung TAM frequency

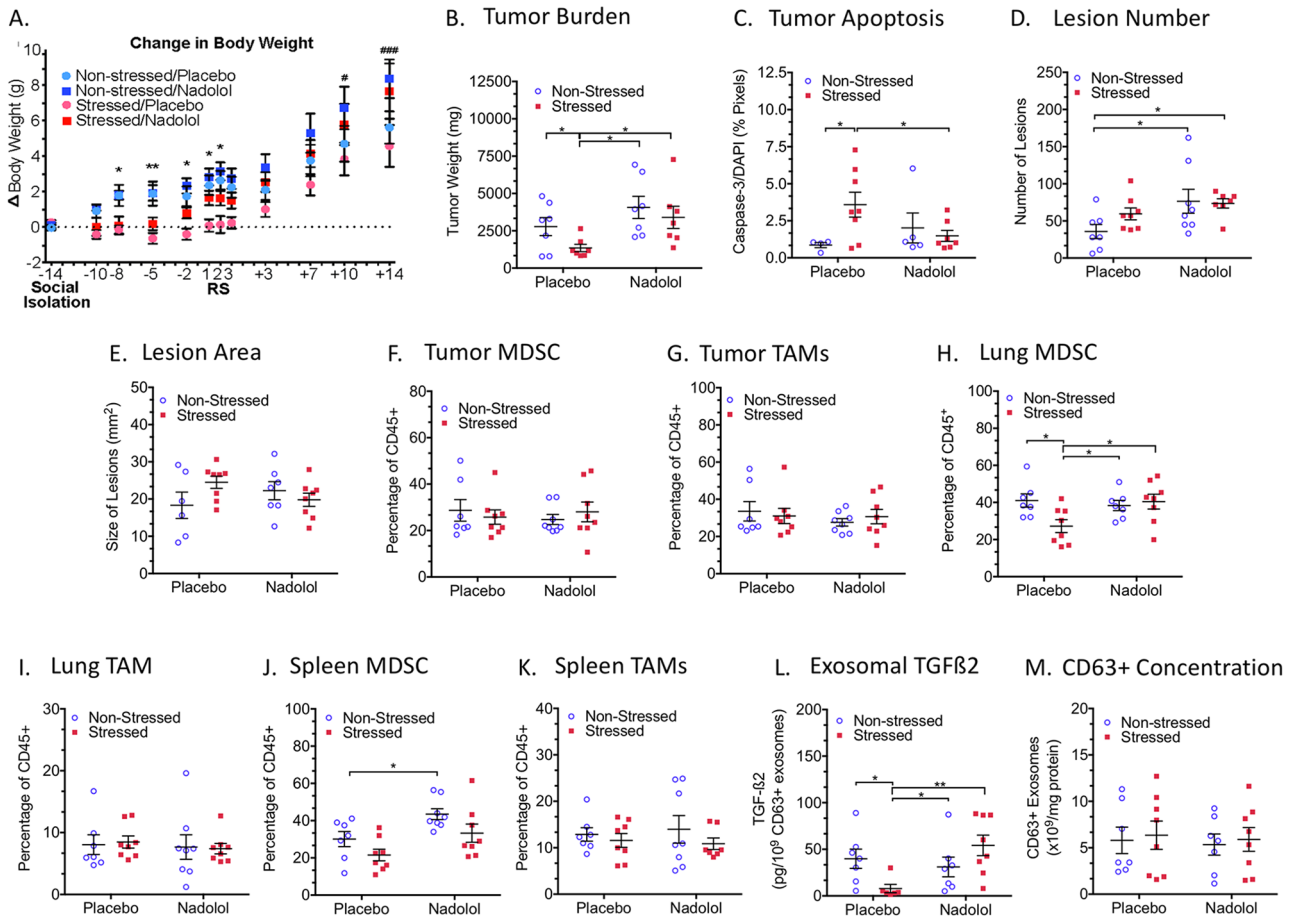


Figure 5. Nadolol treatment prior to stress exposure in MMTV-PyMT mice. (A) Change in body weight (Δ) relative to 1 day before social isolation. (B) Total tumor burden at 3 time points after restraint stress. (C) Tumor apoptosis by quantification of cleaved caspase 3 in tumor sections. (D) Metastatic lesion number and (E) area in H&E-stained sections. Frequency of tumor (F) MDSC and (G) TAM; lung (H) MDSC and (I) TAM; spleen (J) MDSC and (K) TAMs; (L) exosomal TGF β 2 normalized to CD63+ eosomes; (M) concentration of CD63+ exosomes. Individual responses are indicated. Results are expressed as mean \pm SEM. Statistical analyses: Holm-Sidak multiple comparison post-hoc test comparing non-stressed and stressed groups at the corresponding time points, * $p < 0.05$.

was not altered by stress (stress, $P = .9$; Stress \times Nadolol Interaction, $P = .8$; Figure 5I). In the spleen, stress significantly reduced splenic MDSCs independent of nadolol treatment (Figure 5J; stress, $P = .020$; stress by nadolol interaction, $P = .8$), but spleen TAM frequency was not significantly altered by stress (Figure 5K, stress, $P = .3$; Stress \times Nadolol Interaction, $P = .7$). For exosomal TGF- β 2 content, nadolol treatment blocked the effect of stress (Figure 5L, stress, $P = .7$; Stress \times Nadolol Interaction, $P = .01$). These results indicate stress exposure acted through β -AR to inhibit some, but not all, systemic mechanisms associated with tumor growth.

By 2-way ANOVA, significant main effects of nadolol treatment were detected for tumor burden (Figure 5B; $P = .02$), number of lung metastases (Figure 5D; $P = .02$), and splenic MDSC (Figure 5J; $P = .003$). Comparing within the non-stressed groups, the metastatic lesion number and splenic MDSCs were significantly elevated with nadolol treatment compared with placebo based on post hoc analysis (Figure 5D and J). Tumor burden in the nonstressed groups was non-significantly elevated by nadolol treatment (Figure 5B, t test,

$P = .14$). These results demonstrate that β -blockade with nadolol in nonstressed MMTV-PyMT mice increased tumor progression in association with increased frequency of splenic MDSCs, implying that β -AR signaling inhibits these processes in MMTV-PyMT mice.

Discussion

In preclinical models of breast cancer, psychological stress has been linked to tumor progression and metastasis through β -AR activation. Using MMTV-PyMT mice, a spontaneous model of metastatic hormone receptor-positive (ER+/PR+/Her2-Neu+) breast cancer, we have demonstrated that chronic stress exposure reduced primary tumor growth with little impact on metastasis. The stressor, social isolation combined with an acute restraint stress exposure, elicited SNS and HPA axis activation throughout tumor progression. The stress-induced decrease in tumor burden was associated with increased apoptosis within the tumor and suppression of progression-supporting pathways outside the tumor, including reduced frequency of immunosuppressive lung and spleen MDSCs and

decreased circulating exosome TGF- β 2 content. Stress-induced tumor inhibition was prevented by chronic β -blockade with nadolol, a non-selective β -AR antagonist that does not cross the blood-brain barrier, indicating that the tumor inhibitory effects of stress required peripheral β -AR signaling. Unexpectedly, in non-stressed MMTV-PyMT mice, chronic nadolol increased tumor burden, lung metastasis, and splenic MDSC frequency. Together, these results demonstrate that β -AR signaling constrains tumor growth in MMTV-PyMT mice and challenges the narrative that stress acts via β -AR signaling solely to drive tumor progression.

The dual stressor markedly activated the SNS and HPA axis in MMTV-PyMT mice

In our preliminary studies in MMTV-PyMT mice, social isolation (single housing) alone did not increase mammary tumor growth, nor did social isolation consistently elevate tumor or spleen NE or NMN. We speculated habituation to single housing lessened the impact of social isolation on tumor development. To counter habituation, we exposed singly housed mice to an acute stressor. Exposure of isolated mice to an acute stressor has been demonstrated to produce a greater stress neurohormone response compared with isolation alone.^{3,4,48,49} Such a “dual stressor” paradigm may also more closely model the experience of living with an underlying stressor (breast cancer diagnosis) punctuated by additional stressors including biopsy, surgery, and waiting for test results compared with a homotypic stressor. We chose to administer 3 2-hour daily restraint stress sessions, based on increased magnitude and duration of neurohormonal responses observed in non-tumor-bearing mice exposed repeatedly to 2-hour restraint sessions⁵⁰ without accompanying weight loss. MMTV-PyMT mice exposed to the dual stressor displayed heightened plasma CORT and elevated splenic NMN, indicative of HPA axis and SNS activation, as late as 3 weeks after restraint stress exposure without long-lasting weight loss.

The stress-induced reduction in tumor growth was not associated with reduced metastatic lesions in the lung, the primary metastatic site in MMTV-PyMT mice. This result is counter to the report by Chen et al⁵⁷ showing a stress-induced increase in metastatic lesions in MMTV-PyMT mice using a 4-week exposure to unpredictable stress. In this report, prometastatic pathways were activated in the lung with stress exposure, including increased frequency of TAMs. We demonstrated here reduced lung MDSC 2 weeks post-restraint, but lung TAMs were not significantly altered. With our stress paradigm employed, the inability to detect a stress-induced increase in metastatic lesions may have been countered by stress-induced reduction tumor growth and associated activation of tumor inhibitor pathways.

Stress-induced tumor inhibitory mechanisms

Potential immune and non-immune tumor mechanisms underlying the stress-induced reduction in tumor burden

were investigated. Cleaved caspase-3 is a marker of increased apoptosis-mediated cell death and is used as a tumor indicator of therapeutic responsiveness in the clinical setting.⁵⁶ Stressor exposure increased tumor cleaved caspase-3 expression, and the effect was blocked by nadolol, a non-selective β -AR antagonist, implicating β -AR activation in stress-induced tumor inhibition. Thus, increased cell death may explain the stress-induced reduction in tumor burden in MMTV-PyMT mice. Nonetheless, direct induction of apoptosis by β -AR signaling is not consistent with reports that stress⁵⁸ and tumor cell β -AR signaling⁵⁹ augment antiapoptotic pathways to increase tumor growth. Based on the lack of evidence for stress-induced NE release within the tumor, we infer that extratumoral β -AR activation indirectly increased tumor cleaved caspase-3 expression. Furthermore, because nadolol does not cross the blood-brain barrier, we conclude that activation of peripheral, and not central, β -AR elicited stress-induced tumor cleaved caspase-3.

Based on stress-induced elevated CORT levels, we speculate that glucocorticoid receptor activation may have also inhibited tumor growth. This is supported by reports from Pan and colleagues^{60,61} demonstrating an association between glucocorticoid activation and improved outcomes in ER+, but not ER-, breast tumors. The divergence in tumor outcome with glucocorticoid receptor activation observed in patients with breast cancer and the stress-induced tumor inhibition demonstrated here suggest that breast cancer receptor subtype may dictate the response to chronic stress. This possibility will require systematic investigation including other preclinical models of ER+ breast cancer.

Stress exposure did not significantly affect other components of the tumor microenvironment that regulate tumor growth and progression, including immune- and inflammatory-related cytokines and chemokines and tumor infiltration of F4/80+ TAM or CD11b+Gr-1+ MDSCs. Stress exposure did not modify the tumor extracellular matrix, as reported by SHG-emitting collagen, as hypothesized based our previous report demonstrating increased NE availability altered orthotopic tumor SHG-producing fibrillar collagen.⁴³ Stress exposure transiently induced tumor proangiogenic factor VEGF early in tumor development; however, this elevated VEGF was not maintained over time. The inability to detect stress-induced alterations in tumor cytokines, immune populations, and extracellular matrix was unexpected because we demonstrated here β -AR signaling capacity in R221a cells originating from MMTV-PyMT tumors. Furthermore, sympathetic innervation of MMTV-PyMT tumors⁵³ suggests SNS activation and subsequent NE release can directly target cells within the tumor. Nonetheless, we were unable to detect stress-induced sympathetic NE release in MMTV-PyMT tumors (tumor NMN), despite concomitant peripheral sympathetic activation as measured by increased NMN in the spleen (Figure 1D and E). The inability to detect stress-associated

alterations within the tumor is consistent with the lack of evidence for elevated tumor NMN.

Systemic responses to stress inhibited by stress exposure via β -AR signaling

We also demonstrated systemic protumor pathways sensitive to stressor exposure in MMTV-PyMT mice. Tumor cells drive recruitment and expansion of MDSCs in the spleen that infiltrate tumors to suppress antitumor immunity and promote tumor growth.⁶² In association with reduced tumor burden, stress exposure reduced the frequency of MDSCs in the spleen and lung. β -blockade prevented stress-induced MDSC reduction in the lung, but not in the spleen. These results imply that SNS regulation and β -AR signaling of MDSC recruitment and expansion in the spleen is distinct from processes regulating the frequency of MDSCs in the lung. Yet tumor MDSC frequency was not reduced, suggesting that stressor exposure did not modify MDSC recruitment and infiltration into the tumor, and is consistent with no changes in chemokines, such as CCL2, within the tumor that recruit these cells.

Another tumor-driven response that can be measured systemically is the production of circulating exosomes. To our knowledge, the impact of stressor exposure on exosomes in the context of cancer has yet to be investigated. We found that in circulating exosomes isolated from MMTV-PyMT mice, TGF- β_2 , a predominant cytokine in these exosomes, was reduced by stress exposure, and β -AR blockade prevented this suppression. These results provide proof-of-principle that circulating exosomes are sensitive to β -AR signaling and therefore may be useful as readily accessible biomarkers of stress-modulated tumor progression. It is not known from this study whether the stress-blunted exosomal TGF- β content directly contributed to the tumor-suppressive effects of stress or whether it was secondary to reduced tumor growth. It was also not determined whether the isolated circulating exosomes originated from the tumor or host stromal cells.

Chronic nadolol blocked stress-induced tumor outcomes but promoted tumor progression in the absence of stress exposure

Unexpectedly, in non-stressed MMTV-PyMT mice, nadolol treatment increased tumor burden, number of lung metastases, and splenic MDSC frequency. We chose nadolol because it is used clinically and does not cross the blood-brain barrier.⁴⁰ Furthermore, nadolol displays little intrinsic sympathomimetic activity or biased agonism, features of many β -blockers.⁴⁰ Biased agonists, including the commonly used β -blocker propranolol, block ligand-induced classical β -AR signaling (G α s/adenylate cyclase/cAMP) through a structural conformation that also favors signaling through alternative pathways, including the β -arrestin/mitogen-activated protein kinase/extracellular signal-regulated kinase 1/2 pathway.^{63,64} β -blockers that

display biased agonism have been demonstrated to have clinically distinct and opposing effects by activating alternative pathways,⁶⁵⁻⁶⁷ something we wanted to avoid. Another characteristic of many β -blockers, including nadolol, is inverse agonism. β -blockers with inverse agonist activity preferentially stabilize the β -AR structure in a resting conformation that not only blocks ligand signaling but also reduces constitutive β -AR activation.^{64,68} Our choice of nadolol eliminates the potential confounds of intrinsic sympathetic activity or biased agonism, but inverse agonism may explain the unexpected effects of nadolol in nonstressed MMTV-PyMT mice.

We also demonstrated here a link between stress exposure and systemic MDSCs. The finding that nadolol treatment in nonstressed mice increased splenic MDSC frequency suggests that β -AR signaling inhibits MDSC accumulation in the spleen under baseline conditions in MMTV-PyMT mice. This interpretation is consistent with the demonstration that removal of splenic sympathetic innervation increased MDSCs in the spleen and accelerated tumor development.⁶⁹ We speculate that in nonstressed MMTV-PyMT mice, β -AR signaling acts to constrain tumor growth and progression in part by regulation of MDSC expansion or migration. Nadolol treatment removed a tumor-suppressive brake by increasing splenic MDSC and promoting tumor growth and metastasis, as observed here. Together, these results support the conclusion that β -AR stimulation can activate tumor-suppressive mechanisms in MMTV-PyMT mice.

Conclusions

Despite recent advancements identifying mechanisms underlying stress regulation of cancer progression, a review of historical literature reveals significant complexity in psychosocial stress modulation of tumor progression. Throughout the 1960s and 1970s, a number of studies demonstrated differential regulation of tumor progression, depending on factors such as stressor type and chronicity, tumor model, and timing of stress exposure in tumor progression (reviewed in previous studies^{70,71}). Even more recently, Dhabhar and colleagues^{72,73} demonstrated that acute stress inhibited, but chronic stress exacerbated, squamous cell carcinoma development. Our results also imply that psychosocial stress may not exclusively promote tumor progression or metastasis-promoting pathways in cancer. Stress-induced tumor inhibition needs to be better understood to incorporate β -blockers and other therapies that block the stress response as an option in the treatment of cancer.

Acknowledgements

We would like to thank Tracy Bubel for exemplary technical assistance with tissue sectioning and histology, Karen Bentley of the University of Rochester Medical Center (URMC) Electron Microscope Research Core, as well as Tim Bushnell and Matt Cochran of the URMC Flow Cytometry Core. We are also grateful to Seth W. Perry, PhD, and Grayson O. Sipe, PhD, for insightful conversations and commentary on this article.

Author Contributions

RPD, KSM, and EBB designed the studies. RPD, KAB, DKB, PS, ZX, and LC conducted the experiments. RPD analyzed the experimental data. RPD, KSM, and EBB prepared the article. All authors edited and approved the final article.

ORCID iD

Edward B Brown  <https://orcid.org/0000-0002-5367-5330>

Supplemental Material

Supplemental material for this article is available online.

REFERENCES

- DeSantis C, Ma J, Bryan L, Jemal A. Breast cancer statistics, 2013. *CA Cancer Clin.* 2014;64:52-62. doi:10.3322/caac.21203.
- Hinzey A, Gaudier-Diaz MM, Lustberg MB, DeVries AC. Breast cancer and social environment: getting by with a little help from our friends. *Breast Cancer Res.* 2016;18:54. doi:10.1186/s13058-016-0700-x.
- Hermes GL, Delgado B, Tretiakova M, et al. Social isolation dysregulates endocrine and behavioral stress while increasing malignant burden of spontaneous mammary tumors. *Proc Natl Acad Sci USA.* 2009;106:22393-22398. doi:10.1073/pnas.0910753106.
- Williams JB, Pang D, Delgado B, et al. A model of gene-environment interaction reveals altered mammary gland gene expression and increased tumor growth following social isolation. *Cancer Prev Res.* 2009;2:850-861. doi:10.1158/1940-6207.CAPR-08-0238.
- Sloan EK, Priceman SJ, Cox BF, et al. The sympathetic nervous system induces a metastatic switch in primary breast cancer. *Cancer Res.* 2010;70:7042-7052. doi:10.1158/0008-5472.CAN-10-0522.
- Thaker PH, Han LY, Kamat AA, et al. Chronic stress promotes tumor growth and angiogenesis in a mouse model of ovarian carcinoma. *Nat Med.* 2006;12:939-944.
- Le CP, Nowell CJ, Kim-Fuchs C, et al. Chronic stress in mice remodels lymph vasculature to promote tumour cell dissemination. *Nat Commun.* 2016;7:10634. doi:10.1038/ncomms10634.
- Madden KS, Szpunar MJ, Brown EB. Early impact of social isolation and breast tumor progression in mice. *Brain Behav Immun.* 2013;30:S135-S141. doi:10.1016/j.bbi.2012.05.003.
- Volden PA, Conzen SD. The influence of glucocorticoid signaling on tumor progression. *Brain Behav Immun.* 2013;30:S26-S31. doi:10.1016/j.bbi.2012.10.022.
- Ben-Eliyahu S, Page GG, Yirmiya R, Shakhar G. Evidence that stress and surgical interventions promote tumor development by suppressing natural killer cell activity. *Int J Cancer.* 1999;80:880-888.
- Shakhar G, Ben-Eliyahu S. In vivo β -adrenergic stimulation suppresses natural killer activity and compromises resistance to tumor metastasis in rats. *J Immunol.* 1998;160:3251-3258.
- Chang A, Le CP, Walker AK, et al. β 2-Adrenoceptors on tumor cells play a critical role in stress-enhanced metastasis in a mouse model of breast cancer. *Brain Behav Immun.* 2016;57:106-115. doi:10.1016/j.bbi.2016.06.011.
- Pon CK, Lane JR, Sloan EK, Halls ML. The β 2-adrenoceptor activates a positive cAMP-calcium feedforward loop to drive breast cancer cell invasion. *FASEB J.* 2016;30:1144-1154. doi:10.1096/fj.15-277798.
- Sood AK, Armaiz-Pena GN, Halder J, et al. Adrenergic modulation of focal adhesion kinase protects human ovarian cancer cells from anoikis. *J Clin Invest.* 2010;120:1515-1523. doi:10.1172/JCI40802.
- Chida Y, Hamer M, Wardle J, Steptoe A. Do stress-related psychosocial factors contribute to cancer incidence and survival. *Nat Clin Pract Oncol.* 2008;5:466-475. doi:10.1038/nponc1134.
- Lillberg K, Verkasalo PK, Kaprio J, Teppo L, Helenius H, Koskenvuo M. Stressful life events and risk of breast cancer in 10,808 women: a cohort study. *Am J Epidemiol.* 2003;157:415-423.
- Antonova L, Aronson K, Mueller CR. Stress and breast cancer: from epidemiology to molecular biology. *Breast Cancer Res.* 2011;13:208. doi:10.1186/bcr2836.
- Melhem-Bertrandt A, Chavez-Macgregor M, Lei X, et al. Beta-blocker use is associated with improved relapse-free survival in patients with triple-negative breast cancer. *J Clin Oncol.* 2011;29:2645-2652. doi:10.1200/JCO.2010.33.4441.
- Barron TI, Connolly RM, Sharp L, Bennett K, Visvanathan K. Beta blockers and breast cancer mortality: a population-based study. *J Clin Oncol.* 2011;29:2635-2644. doi:10.1200/JCO.2010.33.5422.
- Armaiz-Pena GN, Allen JK, Cruz A, et al. Src activation by beta-adrenoreceptors is a key switch for tumour metastasis. *Nat Commun.* 2013;4:1403. doi:10.1038/ncomms2413.
- Botteri E, Munzone E, Rotmensz N, et al. Therapeutic effect of beta-blockers in triple-negative breast cancer postmenopausal women. *Breast Cancer Res Treat.* 2013;140:567-575. doi:10.1007/s10549-013-2654-3.
- Fryzek JP, Poulsen AH, Lipworth L, et al. A cohort study of antihypertensive medication use and breast cancer among Danish women. *Breast Cancer Res Treat.* 2006;97:231-236. doi:10.1007/s10549-005-9091-x.
- Cardwell CR, Coleman HG, Murray LJ, Entschladen F, Powe DG. Beta-blocker usage and breast cancer survival: a nested case-control study within a UK clinical practice research datalink cohort. *Int J Epidemiol.* 2013;42:1852-1861. doi:10.1093/ije/dyt196.
- Shah SM, Carey IM, Owen CG, Harris T, Dewilde S, Cook DG. Does beta-adrenoceptor blocker therapy improve cancer survival? Findings from a population-based retrospective cohort study. *Br J Clin Pharmacol.* 2011;72:157-161. doi:10.1111/j.1365-2125.2011.03980.x.
- Sorensen GV, Ganz PA, Cole SW, et al. Use of beta-blockers, angiotensin-converting enzyme inhibitors, angiotensin II receptor blockers, and risk of breast cancer recurrence: a Danish nationwide prospective cohort study. *J Clin Oncol.* 2013;31:2265-2272. doi:10.1200/JCO.2012.43.9190.
- Skog J, Wurdinger T, van Rijn S, et al. Glioblastoma microvesicles transport RNA and proteins that promote tumour growth and provide diagnostic biomarkers. *Nat Cell Biol.* 2008;10:1470-1476. doi:10.1038/ncb1800.
- Costa-Silva B, Aiello NM, Ocean AJ, et al. Pancreatic cancer exosomes initiate pre-metastatic niche formation in the liver. *Nat Cell Biol.* 2015;17:816-826. doi:10.1038/ncb3169.
- Melo SA, Sugimoto H, O'Connell JT, et al. Cancer exosomes perform cell-independent microRNA biogenesis and promote tumorigenesis. *Cancer Cell.* 2014;26:707-721. doi:10.1016/j.ccell.2014.09.005.
- Melo SA, Luecke LB, Kahler C, et al. Glypican-1 identifies cancer exosomes and detects early pancreatic cancer. *Nature.* 2015;523:177-182. doi:10.1038/nature14581.
- Peinado H, Aleckovic M, Lavotshkin S, et al. Melanoma exosomes educate bone marrow progenitor cells toward a pro-metastatic phenotype through MET. *Nat Med.* 2012;18:883-891. doi:10.1038/nm.2753.
- Colombo M, Raposo G, Thery C. Biogenesis, secretion, and intercellular interactions of exosomes and other extracellular vesicles. *Annu Rev Cell Dev Biol.* 2014;30:255-289. doi:10.1146/annurev-cellbio-101512-122326.
- Antonyak MA, Li B, Boroughs LK, et al. Cancer cell-derived microvesicles induce transformation by transferring tissue transglutaminase and fibronectin to recipient cells. *Proc Natl Acad Sci USA.* 2011;108:4852-4857. doi:10.1073/pnas.1017667108.
- Ringuette Goulet C, Bernard G, Tremblay S, Chabaud S, Bolduc S, Pouliot F. Exosomes induce fibroblast differentiation into cancer-associated fibroblasts through TGF β signaling. *Mol Cancer Res.* 2018;16:1196-1204. doi:10.1158/1541-7786.MCR-17-0784.
- Szajnik M, Derbis M, Lach M, et al. Exosomes in plasma of patients with ovarian carcinoma: potential biomarkers of tumor progression and response to therapy. *Gynecol Obstet.* 2013;4:3. doi:10.4172/2161-0932.S4-003.
- Webber JP, Spary LK, Sanders AJ, et al. Differentiation of tumour-promoting stromal myofibroblasts by cancer exosomes. *Oncogene.* 2015;34:290-302. doi:10.1038/onc.2013.560.
- Beninson LA, Brown PN, Loughridge AB, et al. Acute stressor exposure modifies plasma exosome-associated heat shock protein 72 (Hsp72) and microRNA (miR-142-5p and miR-203). *PLoS ONE.* 2014;9:e108748. doi:10.1371/journal.pone.0108748.
- Padro CJ, Shawler TM, Gormley MG, Sanders VM. Adrenergic regulation of IgE involves modulation of CD23 and ADAM10 expression on exosomes. *J Immunol.* 2013;191:5383-5397. doi:10.4049/jimmunol.1301019.
- Lin EY, Jones JG, Li P, et al. Progression to malignancy in the polyoma middle T oncoprotein mouse breast cancer model provides a reliable model for human diseases. *Am J Pathol.* 2003;163:2113-2126. doi:10.1016/S0002-9440(10)63568-7.
- Sorge RE, Martin LJ, Isbester KA, et al. Olfactory exposure to males, including men, causes stress and related analgesia in rodents. *Nat Methods.* 2014;11:629-632. doi:10.1038/nmeth.2935.
- Reiter MJ. Cardiovascular drug class specificity: beta-blockers. *Prog Cardiovasc Dis.* 2004;47:11-33.
- Madden KS, Felten DL. Beta-adrenoceptor blockade alters thymocyte differentiation in aged mice. *Cell Mol Biol.* 2001;47:189-196.
- Dobbs CM, Vasquez M, Glaser R, Sheridan JF. Mechanisms of stress-induced modulation of viral pathogenesis and immunity. *J Neuroimmunol.* 1993;48:151-160.
- Szpunar MJ, Burke KA, Dawes RP, Brown EB, Madden KS. The antidepressant desipramine and α 2-adrenergic receptor activation promote breast tumor progression in association with altered collagen structure. *Cancer Prev Res.* 2013;6:1262-1272. doi:10.1158/1940-6207.CAPR-13-0079.

44. Perfetto SP, Chattopadhyay PK, Roederer M. Seventeen-colour flow cytometry: unravelling the immune system. *Nat Rev Immunol.* 2004;4:648-655. doi:10.1038/nri1416.
45. Thery C, Zitvogel L, Amigorena S. Exosomes: composition, biogenesis and function. *Nat Rev Immunol.* 2002;2:569-579. doi:10.1038/nri855.
46. Martin MD, Carter KJ, Jean-Philippe SR, et al. Effect of ablation or inhibition of stromal matrix metalloproteinase-9 on lung metastasis in a breast cancer model is dependent on genetic background. *Cancer Res.* 2008;68:6251-6259. doi:10.1158/0008-5472.CAN-08-0537.
47. Madden KS, Szpunar MJ, Brown EB. beta-Adrenergic receptors (beta-AR) regulate VEGF and IL-6 production by divergent pathways in high beta-AR-expressing breast cancer cell lines. *Breast Cancer Res Treat.* 2011;130:747-758. doi:10.1007/s10549-011-1348-y.
48. Bartolomucci A, Palanza P, Sacerdote P, et al. Individual housing induces altered immuno-endocrine responses to psychological stress in male mice. *Psychoneuroendocrinology.* 2003;28:540-558.
49. Dronjak S, Gavrilovic L, Filipovic D, Radojic MB. Immobilization and cold stress affect sympatho-adrenomedullary system and pituitary-adrenocortical axis of rats exposed to long-term isolation and crowding. *Physiol Behav.* 2004;81:409-415. doi:10.1016/j.physbeh.2004.01.011.
50. Sadler AM, Bailey SJ. Repeated daily restraint stress induces adaptive behavioural changes in both adult and juvenile mice. *Physiol Behav.* 2016;167:313-323. doi:10.1016/j.physbeh.2016.09.014.
51. Voorhees JL, Tarr AJ, Wohleb ES, et al. Prolonged restraint stress increases IL-6, reduces IL-10, and causes persistent depressive-like behavior that is reversed by recombinant IL-10. *PLoS ONE.* 2013;8:e58488. doi:10.1371/journal.pone.0058488.
52. Eisenhofer G, Kopin IJ, Goldstein DS. Catecholamine metabolism: a contemporary view with implications for physiology and medicine. *Pharmacol Rev.* 2004;56:331-349. doi:10.1124/pr.56.3.1.
53. Szpunar MJ, Belcher EK, Dawes RP, Madden KS. Sympathetic innervation, norepinephrine content, and norepinephrine turnover in orthotopic and spontaneous models of breast cancer. *Brain Behav Immun.* 2016;53:223-233. doi:10.1016/j.bbi.2015.12.014.
54. Wang Y, Lu Y, Yu D, et al. Enhanced resistance of restraint-stressed mice to sepsis. *J Immunol.* 2008;181:3441-3448.
55. Burke K, Tang P, Brown E. Second harmonic generation reveals matrix alterations during breast tumor progression. *J Biomed Opt.* 2013;18:31106. doi:10.1117/1.JBO.18.3.031106.
56. Tham YL, Gomez LF, Mohsin S, et al. Clinical response to neoadjuvant docetaxel predicts improved outcome in patients with large locally advanced breast cancers. *Breast Cancer Res Treat.* 2005;94:279-284. doi:10.1007/s10549-005-9020-z.
57. Chen H, Liu D, Guo L, Cheng X, Guo N, Shi M. Chronic psychological stress promotes lung metastatic colonization of circulating breast cancer cells by decorating a pre-metastatic niche through activating beta-adrenergic signaling. *J Pathol.* 2018;244:49-60. doi:10.1002/path.4988.
58. Eng JW, Reed CB, Kokolus KM, et al. Housing temperature-induced stress drives therapeutic resistance in murine tumour models through beta2-adrenergic receptor activation. *Nat Commun.* 2015;6:6426. doi:10.1038/ncomms7426.
59. Sastry KS, Karpova Y, Prokopovich S, et al. Epinephrine protects cancer cells from apoptosis via activation of cAMP-dependent protein kinase and BAD phosphorylation. *J Biol Chem.* 2007;282:14094-14100. doi:10.1074/jbc.M611370200.
60. Pan D, Kocherginsky M, Conzen SD. Activation of the glucocorticoid receptor is associated with poor prognosis in estrogen receptor-negative breast cancer. *Cancer Res.* 2011;71:6360-6370. doi:10.1158/0008-5472.CAN-11-0362.
61. West DC, Pan D, Tonsing-Carter EY, et al. GR and ER coactivation alters the expression of differentiation genes and associates with improved ER+ breast cancer outcome. *Mol Cancer Res.* 2016;14:707-719. doi:10.1158/1541-7786.MCR-15-0433.
62. McAllister SS, Weinberg RA. The tumour-induced systemic environment as a critical regulator of cancer progression and metastasis. *Nat Cell Biol.* 2014;16:717-727. doi:10.1038/ncb3015.
63. Wisler JW, DeWire SM, Whalen EJ, et al. A unique mechanism of beta-blocker action: carvedilol stimulates beta-arrestin signaling. *Proc Natl Acad Sci USA.* 2007;104:16657-16662. doi:10.1073/pnas.0707936104.
64. Thanawala VJ, Forkuo GS, Stallaert W, Leff P, Bouvier M, Bond R. Ligand bias prevents class equality among beta-blockers. *Curr Opin Pharmacol.* 2014;16:50-57. doi:10.1016/j.coph.2014.03.002.
65. Hanania NA, Singh S, El-Wali R, et al. The safety and effects of the beta-blocker, nadolol, in mild asthma: an open-label pilot study. *Pulm Pharmacol Ther.* 2008;21:134-141. doi:10.1016/j.pupt.2007.07.002.
66. Short PM, Williamson PA, Anderson WJ, Lipworth BJ. Randomized placebo-controlled trial to evaluate chronic dosing effects of propranolol in asthma. *Am J Respir Crit Care Med.* 2013;187:1308-1314. doi:10.1164/rccm.201212-2206OC.
67. Thanawala VJ, Valdez DJ, Joshi R, et al. Beta-blockers have differential effects on the murine asthma phenotype. *Br J Pharmacol.* 2015;172:4833-4846. doi:10.1111/bph.13253.
68. Chidiac P, Hebert TE, Valiquette M, Dennis M, Bouvier M. Inverse agonist activity of beta-adrenergic antagonists. *Mol Pharmacol.* 1994;45:490-499.
69. Dubeykovskaya Z, Si Y, Chen X, et al. Neural innervation stimulates splenic TFF2 to arrest myeloid cell expansion and cancer. *Nat Commun.* 2016;7:10517. doi:10.1038/ncomms10517.
70. Sklar LS, Anisman H. Stress and cancer. *Psychol Bull.* 1981;89:369-406.
71. Justice A. Review of the effects of stress on cancer in laboratory animals: importance of time of stress application and type of tumor. *Psychol Bull.* 1985;98:108-138.
72. Dhabhar FS, Saul AN, Daugherty C, Holmes TH, Bouley DM, Oberyszyn TM. Short-term stress enhances cellular immunity and increases early resistance to squamous cell carcinoma. *Brain Behav Immun.* 2010;24:127-137. doi:10.1016/j.bbi.2009.09.004.
73. Saul AN, Oberyszyn TM, Daugherty C, et al. Chronic stress and susceptibility to skin cancer. *J Natl Cancer Inst.* 2005;97:1760-1767. doi:10.1093/jnci/dji401.